Available online at www.sciencedirect.com
SCIENCE DIRECT®
Catalysis Today 97 (2004) 95–101
CATALYSIS TODAY
www.elsevier.com/locate/cattod

Preparation of nano-gold on $K_2La_2Ti_3O_{10}$ for producing hydrogen from photo-catalytic water splitting

Yu-Wei Tai, Jeng-Shiou Chen, Chieh-Chao Yang, Ben-Zu Wan*

Department of Chemical Engineering, National Taiwan University, Taipei, Taiwan 10617, ROC

Received 18 November 2003; received in revised form 6 March 2004; accepted 2 April 2004
Available online 28 July 2004

Abstract

The effects of gold loading (i.e., loading processes and pretreatment procedures) on the perovskite titanate substrate ($K_2La_2Ti_3O_{10}$) for photo-catalytic water splitting were studied. It was found that the gold catalyst prepared from an incipient wetness impregnation process possessed a better activity for water splitting than that prepared from a deposition process. This is because a better crystallinity of $K_2La_2Ti_3O_{10}$ was preserved from the impregnation process than that from the deposition. Moreover, the existence of gold on $K_2La_2Ti_3O_{10}$ can enhance the activity of $K_2La_2Ti_3O_{10}$ for photo-catalytic water splitting. Specially, the activity can be increased significantly, after the reduction of gold ions on $K_2La_2Ti_3O_{10}$ to nano-gold metal through some pretreatment processes studied in this research. When compared with the best metal–titanate catalyst reported in the literature (i.e., $Ni/K_2La_2Ti_3O_{10}$), $Au/K_2La_2Ti_3O_{10}$ possessed a lower hydrogen production rate in UV region and a higher one in vis region. This may be because there is absorption from plasma resonance on the nano-gold surface of $Au/K_2La_2Ti_3O_{10}$ in the visible region, rather than on the surface of $Ni/K_2La_2Ti_3O_{10}$.

Keywords: Water splitting; Photo-catalytic; Au; Perovskite titanate; Hydrogen

1. Introduction

In the past it has been shown that nano-gold can be prepared on various transition metal oxides (such as Fe_2O_3, CoO_x, or TiO_2) [1–3], and on some other catalyst supports (such as zeolite or alumina) [4–7]. Different from the poorly catalytic activity of bulk gold, unique catalytic properties, specially for the oxidation of CO at low temperature and for the epoxidation of propylene, have been found from these catalysts [1–9]; moreover, an unique absorption band around 500 nm wavelength, which is from the surface plasma resonance [10], was observed from some of these nano-gold [11]. Therefore, it is the interest of this research to examine whether the surface and the catalytic properties of nano-gold can provide some influence on the photo-dissociation of water to produce hydrogen and oxygen.

Hydrogen can be utilized as a main energy source for the fuel cell. It is a clean and renewable combustion fuel, if it can be produced mainly from the dissociation of water under sunlight without using fossil energy. Since Fujishima and Honda [12] built up the first TiO_2 system in 1972, a lot of studies for the water splitting under photo have been done. Different catalyst systems have been prepared and investigated. Among them, $SrTiO_3$ [13,14], $K_4Nb_6O_{17}$ [15–20], $BaTi_4O_9$ [21–23], $K_2La_2Ti_3O_{10}$ [24,25], ZrO_2 [26,27], $NaTaO_3$ [28] showed interesting results. From the review of Domen and coworkers [29], it can be found that $Ni/K_2La_2Ti_3O_{10}$ prepared from his research group possessed a remarkable photo-catalytic activity for the production of hydrogen under UV irradiation. The influence of several metals except gold on the photo-activity of $K_2La_2Ti_3O_{10}$ was investigated. It was concluded that the reduced and partially re-oxidized nickel was the best, and the possible mechanism for this photo reaction was proposed. However, it is noticed that gold metal possesses similar values of work function as nickel metal [30]. Moreover, the plasma resonance on nano-gold may provide some influence on the water splitting under visible light. Therefore, in this research, the loading of nano-gold on $K_2La_2Ti_3O_{10}$ was attempted. Different

* Corresponding author. Tel.: +886 2 33663021; fax: +886 2 2362 3040.
E-mail address: benzuwan@ntu.edu.tw (B.-Z. Wan).

0920-5861/$ – see front matter © 2004 Elsevier B.V. All rights reserved.
doi:10.1016/j.cattod.2004.04.054

processes (i.e., deposition and impregnation) for the preparation of gold catalysts were examined. The effect of gold on the photo-catalytic activity of $K_2La_2Ti_3O_{10}$ was investigated. Finally, a preliminary comparison of the activities of nano-gold and the reduced (then partially re-oxidized) nickel for water splitting under UV or visible light were made.

2. Experimental

$K_2La_2Ti_3O_{10}$ powders were synthesized according to the polymer complexing method developed by Ikeda et al. [25]. $Ti(OiPr)_4$, $La(NO_3)_3{\cdot}6H_2O$ and K_2CO_3 were selected as starting materials. The amount of K_2CO_3 was controlled twice excess of stoichiometry in order to compensate for the loss of potassium by volatilization. Ethylene glycol (EG) and methanol were used as the solvents, and citric acid (CA) was used as a complexing agent to stabilize Ti, La, and K ions against water generated during the polymerization between EG and CA. Two methods for the loading of gold on $K_2La_2Ti_3O_{10}$ were used in this study. Au-i/$K_2La_2Ti_3O_{10}$ was prepared by the incipient-wetness impregnation of the chloroauric acid solution ($HAuCl_4{\cdot}3H_2O$, Merck) onto the $K_2La_2Ti_3O_{10}$ powder, and then dried at 60 °C in air overnight. Au-d/$K_2La_2Ti_3O_{10}$ was prepared by the deposition of gold in a chloroauric acid solution, as illustrated in our previous paper [4,5]. The followings are the deposition steps: 4 g of $K_2La_2Ti_3O_{10}$ was charged into a 500 ml of chloroauric acid aqueous solution, which was adjusted to pH 6 before the charging. Under stirring, the solution was heated to 80 °C and maintained at this temperature for 16 h. After filtration, the samples were washed until free from Cl^- ions, as detected by an $AgNO_3$ solution and then dried at 60 °C in air overnight. Moreover, the preparation of nickel on $K_2La_2Ti_3O_{10}$ powders and the pretreatment of this nickel-loaded sample followed the same methods developed by Ikeda et al. [25].

Photo-catalytic reaction for water splitting was carried out in an inner-type irradiation reactor, as shown in Fig. 1. Catalyst (0.3 g) was dispersed in an aqueous KOH solution (0.1 M, 120 ml) by magnetic stirring and was irradiated under vacuum (about 50 Torr) by sixteen monochromic lamps around the reactor. Two light sources were used. One was around 300 ± 50 nm wavelength (21 W for each lamp) in the UV region. The other was around 419 ± 25 nm (24 W for each lamp) in the visible region. Every 60 min during the reaction test, 10 ml of gas sample was taken from the sampling loop of the reactor by a syringe, and was injected into a gas chromatography (molecular sieve 5 A column, Ar as the carrier gas, TCD detector) for the analysis of the products. The hydrogen production rate was determined from the slope of the hydrogen accumulation in the first hour divided by the catalyst weight used in the reaction. Moreover, the catalysts were characterized by temperature programmed reduction (TPR) by hydrogen, by atomic absorption for gold loading (GBC 906), and by UV–vis diffuse reflectance (Hitachi U-3410) for band gap and for the characterization of plasma band of nano-gold. The XRD measurements were carried out on a MAC Science Diffractometer (model MXP-3). The measured half maximum breadth, B_{exp}, of the gold peak at $2\theta = 39^\circ$ was used by Scherrer equation for the estimation of average gold crystal size on $K_2La_2Ti_3O_{10}$. The expression of Scherrer equation [31] using Gaussian–Gaussian approximation is known as:

$$L = \frac{K\lambda}{B\cos\theta}, \quad B^2 = B_{exp}^2 - b^2 \tag{1}$$

where L and θ are the average crystal size and Bragg angle of gold, respectively. B and b are the breadths of intrinsic diffraction profile and instrumental diffraction profile, respectively. The value of b for the MXP-3 Diffractometer is 0.003 arcs. λ is the wavelength of the Cu Kα X-ray source, which is 1.5405 Å. K is the Scherrer constant and is set to be unity. The experimental error for average gold crystal size is ±3 nm.

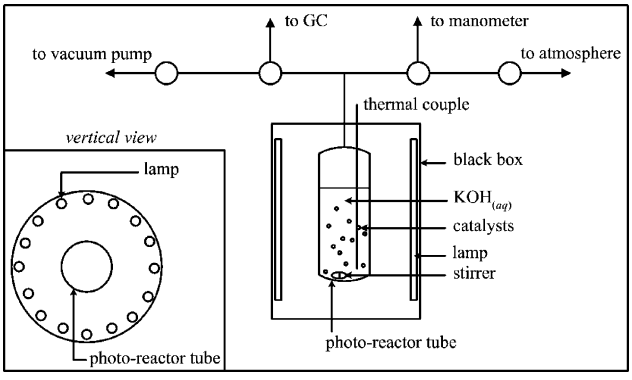

Fig. 1. The apparatus for photo-catalytic reaction.

3. Results and discussion

3.1. Effect of Au loading on $K_2La_2Ti_3O_{10}$

The Au-d/$K_2La_2Ti_3O_{10}$ with different Au loadings were prepared, according to the deposition method. The amounts of three Au loadings were designed originally to be 0.5, 1 and 3wt.%, respectively; however, the resulted Au contents in Au-d/$K_2La_2Ti_3O_{10}$ were about twice of those designed. For example, 1.9 wt.% Au in Au-d/$K_2La_2Ti_3O_{10}$ was measured, in which 1% was designed originally. The increase of Au loading may be because the dissolution of potassium oxides or lanthanum oxides within $K_2La_2Ti_3O_{10}$ into the acidic solution (pH 6 at 80 °C) during deposition. The dissolution caused the weight reduction of $K_2La_2Ti_3O_{10}$. Therefore, it can be observed from the XRD patterns in Fig. 2 that Au-d/$K_2La_2Ti_3O_{10}$ with 1.9 wt.%Au lost a significant crystallinity. The peaks from Au-d/$K_2La_2Ti_3O_{10}$ were weak (peak to noise ratio) and shifted slightly away from those of $K_2La_2Ti_3O_{10}$. Moreover, the BET surface area

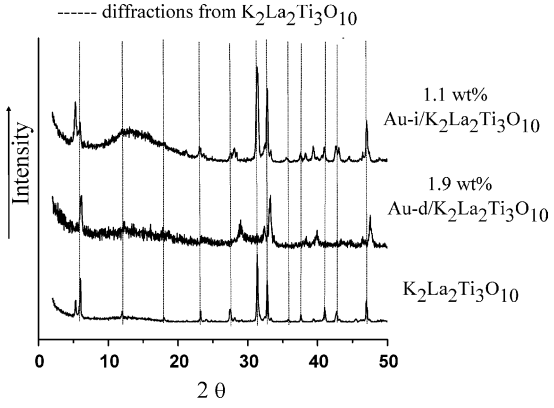

Fig. 2. XRD patterns of Au-i/$K_2La_2Ti_3O_{10}$ with 1.1 wt.%Au, Au-d/$K_2La_2Ti_3O_{10}$ with 1.9 wt.%Au and $K_2La_2Ti_3O_{10}$. All the catalysts were pretreated under H_2 at 200 °C for 2 h.

was increased from 3 m^2/g of $K_2La_2Ti_3O_{10}$ to 30 m^2/g of Au-d/$K_2La_2Ti_3O_{10}$ shown in Fig. 2. Apparently, the dissolution caused opening of pores between the layers of $K_2La_2Ti_3O_{10}$. On the other hand, for photo-decomposition of water on these catalysts, the dependence of hydrogen production rate on the amount of loaded gold on Au-d/$K_2La_2Ti_3O_{10}$ is shown in Fig. 3. Prior to the reaction tests, the catalysts were reduced under hydrogen at 200 °C for 2 h. UV lamp around 300 nm was used for the irradiation during the reaction. From the hydrogen evolution rates, it can be found that the optimal amount of Au loading on Au-d/$K_2La_2Ti_3O_{10}$ for water splitting was 1.9 wt.%. The rate of H_2 evolution increased with the increase of gold loading until 1.9 wt.%; on the other hand, it decreased gradually when the loading was more than 1.9 wt.%. The results strongly indicate that the existence of gold particles can enhance the catalytic property of $K_2La_2Ti_3O_{10}$ for water splitting.

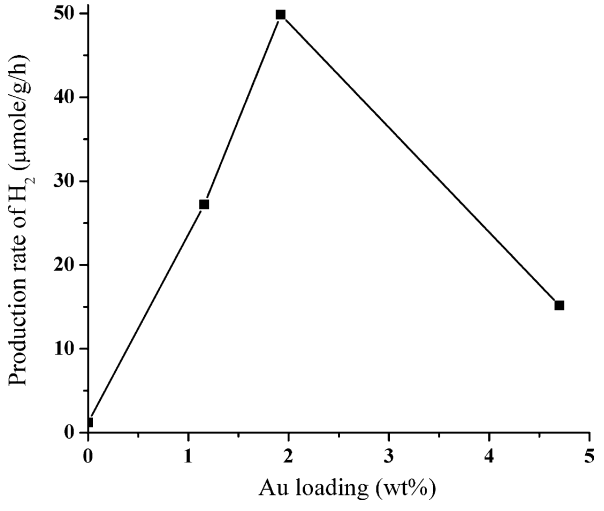

Fig. 3. Effect of gold loading on Au-d/$K_2La_2Ti_3O_{10}$ catalysts for water splitting under 300 nm UV light irradiation. The catalysts were pretreated under H_2 at 200 °C for 2 h.

3.2. Comparison between Au-d/$K_2La_2Ti_3O_{10}$ and Au-i/$K_2La_2Ti_3O_{10}$

For the preparation of Au-i/$K_2La_2Ti_3O_{10}$ by incipient wetness method, the resulted Au content in Au-i/$K_2La_2Ti_3O_{10}$ catalyst was 1.1 wt.%, which was close to 1 wt.% designed originally. Therefore, this sample was compared with Au-d/$K_2La_2Ti_3O_{10}$ loaded with 1.9 wt.%Au, in which 1% was designed originally, and which was the one with the best catalytic activity shown in Fig. 3. Prior to the characterization and the reaction tests, a pretreatment under hydrogen at 200 °C for reducing gold ions to metal was used. Fig. 2 shows the XRD patterns of Au-d/$K_2La_2Ti_3O_{10}$ and Au-i/$K_2La_2Ti_3O_{10}$ along with that of $K_2La_2Ti_3O_{10}$. The peaks at $2\theta = 39^\circ$ from Au-d/$K_2La_2Ti_3O_{10}$ and Au-i/$K_2La_2Ti_3O_{10}$ represent the diffraction of gold crystals. Moreover, it can be observed that Au-i/$K_2La_2Ti_3O_{10}$ of the impregnation sample maintained a crystallinity close to that of $K_2La_2Ti_3O_{10}$, in contrast to a significant loss of crystallinity from Au-d/$K_2La_2Ti_3O_{10}$. Table 1 lists the gold crystal sizes, the band gaps of $K_2La_2Ti_3O_{10}$, Au-i/$K_2La_2Ti_3O_{10}$ and Au-d/$K_2La_2Ti_3O_{10}$. In this table, the influence from several different pretreatment processes were also examined for Au-i/$K_2La_2Ti_3O_{10}$ and will be discussed later; only the samples pretreated at 200 °C under hydrogen (LTR) are compared in this section. It can be found that the gold crystal sizes (calculated from the half peak widths at $2\theta = 39^\circ$ of XRD spectra and according to Scherrer equation) on both Au-i/$K_2La_2Ti_3O_{10}$ and Au-d/$K_2La_2Ti_3O_{10}$ were 44 and 38 nm, respectively, which were close in size and were in the range of nano-gold. The band gap of Au-i/$K_2La_2Ti_3O_{10}$ was close to that of $K_2La_2Ti_3O_{10}$ and was in UV region. However, the band gap of Au-d/$K_2La_2Ti_3O_{10}$ was in the region of visible light, which was significantly lower than that of $K_2La_2Ti_3O_{10}$. The band gap shift of Au-d/$K_2La_2Ti_3O_{10}$ away from that of $K_2La_2Ti_3O_{10}$ is consistent with the data of XRD, which was apparently due to the lattice distortion of $K_2La_2Ti_3O_{10}$ of this gold deposited sample.

For the reaction activity of water splitting shown in Fig. 4, it can be observed that under the irradiation by 300 nm UV light, both Au-i/$K_2La_2Ti_3O_{10}$ and Au-d/$K_2La_2Ti_3O_{10}$ possessed much higher reaction rates than $K_2La_2Ti_3O_{10}$. However, the activity of Au-i/$K_2La_2Ti_3O_{10}$ was higher than that of Au-d/$K_2La_2Ti_3O_{10}$ by about 10 times. Note, both band gaps of Au-i/$K_2La_2Ti_3O_{10}$ and Au-d/$K_2La_2Ti_3O_{10}$ were lower than the energy of 300 nm light source. And both band gaps are higher than the bonding energy for water splitting. The reaction activities from both gold catalysts should have not been so much different. Since the gold crystals on both catalysts were similar in size, and presume they were with similar catalytic properties; therefore, the results from this research indicate that the phase of $K_2La_2Ti_3O_{10}$ for the catalyst loaded with gold was important for photo-catalytic water splitting. The electron and the hole generated in $K_2La_2Ti_3O_{10}$ during the irradiation by light is the main source for the reduction and the oxidation of water.

Table 1
Some physical properties of Au-loaded $K_2La_2Ti_3O_{10}$ and photo-catalytic activities for water splitting

Loaded material[a]	Process of pretreatment[b]	Initial H_2 production rate[c] (μmol/g/h)	Bandgap (nm)	Structure of titanate (from XRD)	Crystal size of Au[d] (nm)
Au-i/$K_2La_2Ti_3O_{10}$	WP	282	360	Y	50
	LTR	821	360	Y	44
	HTR	795	360	Y	56
	C	769	360	Y	44
	HTR/C	449	365	Y	52
	HTR/C/LTR	705	365	Y	53
	HTR′/C/LTR	841	370	Y	44
Au-d/$K_2La_2Ti_3O_{10}$	LTR	89	410	N	38
$K_2La_2Ti_3O_{10}$	~	1.2	345	Y	–

[a] The Au loading is 1.1 wt.% in Au-i/$K_2La_2Ti_3O_{10}$ and 1.9 wt.% in Au-d/$K_2La_2Ti_3O_{10}$. Reaction condition: 0.3 g of catalyst in 0.1 M of 120 ml KOH solution under 300 nm UV irradiation.
[b] Different pretreatment process for 2 h. WP, without pre-treatment; LTR, reduction under H_2 at 200 °C; HTR, reduction at 600 °C; HTR′, reduction at 500 °C; *C*, calcination under air at 400 °C.
[c] The initial rate was calculated from the hydrogen production per catalyst weight in the first hour.
[d] The crystal size was calculated by Sherrer's equation from the XRD peak at Au (2θ =39°).

It is likely that nano-gold on $K_2La_2Ti_3O_{10}$ is used for reducing the recombination rate of electron and hole in $K_2La_2Ti_3O_{10}$; otherwise, the high recombination rate would cause a low activity for water splitting. Moreover, the lattice distortion and the loss of crystallinity of $K_2La_2Ti_3O_{10}$ in Au-d/$K_2La_2Ti_3O_{10}$ simply caused this sample with much less efficiency for the generation of electron and hole during the irradiation by light.

Because Au-i/$K_2La_2Ti_3O_{10}$ of the impregnation sample possessed a much higher photo-catalytic activity than Au-d/$K_2La_2Ti_3O_{10}$ of the deposition sample, only Au-i/$K_2La_2Ti_3O_{10}$ was studied in the later sections of this research. Several different catalyst pretreatment processes were applied for the improvement of the activity of nano-gold.

3.3. Pretreatment effects on Au-i/$K_2La_2Ti_3O_{10}$

Fig. 5 presents the results of TPR by hydrogen from a fresh Au-i/$K_2La_2Ti_3O_{10}$ prior to any pretreatment. It can be observed that a major reduction band from gold ions occurred at the temperature about 180 °C. When the temperatures were higher than 200 °C, some more small reduction bands were found. Several were between 300 and 400 °C, and some broad ones were between 400 and 600 °C. The major reduction band at 180 °C is close to the reduction temperature for gold chloride impregnated on Y type zeolite [32]. This indicates that gold chloride impregnated on $K_2La_2Ti_3O_{10}$ was still in the form of this precursor; otherwise, lower reduction temperatures should have been found [4,5,11,32]. Because chloride is a poison for the catalytic property of nano-gold, therefore, several different pretreatment procedures at high temperatures [33] were applied on Au-i/$K_2La_2Ti_3O_{10}$ for the removal of chloride on the surface. Nevertheless, it was noticed that too high temperatures might cause the sintering of gold on the

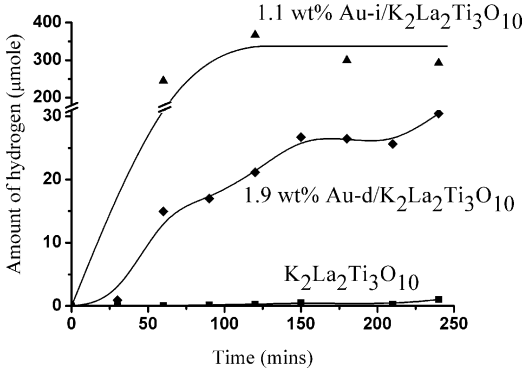

Fig. 4. Reaction time vs. amount of hydrogen accumulated from photo-catalytic water splitting over 0.3 g each of Au-i/$K_2La_2Ti_3O_{10}$, Au-d/$K_2La_2Ti_3O_{10}$ and $K_2La_2Ti_3O_{10}$ under 300 nm UV irradiation.

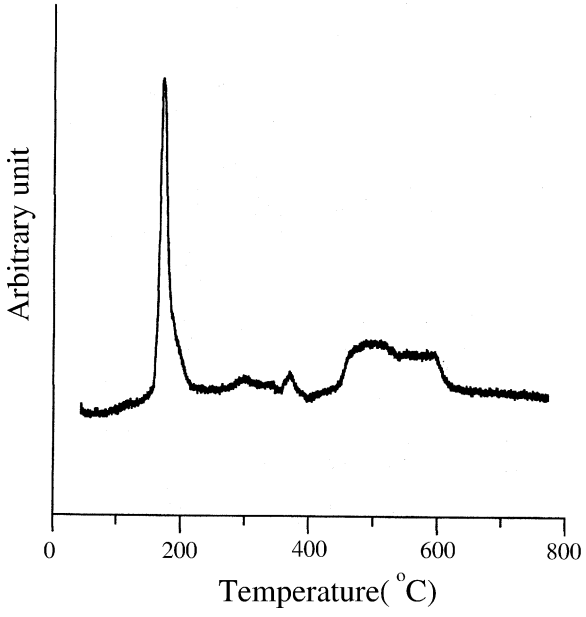

Fig. 5. Temperature programmed reduction (TPR) of fresh Au-i/$K_2La_2Ti_3O_{10}$ with 1.1 wt.% Au, under hydrogen.

supports, which may lower the catalytic activity. Therefore, the effort was made in this research to determine which process was more effective for the pretreatment, in order to obtain a better Au-i/$K_2La_2Ti_3O_{10}$ for the reaction activity.

Since TPR results from the fresh Au-i/$K_2La_2Ti_3O_{10}$ indicate that except the major reduction band around 180 °C, there are small bands between 300 and 400 °C, and between 400 and 600 °C. Therefore, the temperatures between 200 and 600 °C were used for the pretreatment study. The pretreatment was either under hydrogen or under air. The followings are the abbreviation for the different pretreatment processes: LTR, HTR′ and HTR represent the reduction under hydrogen for 2 h at 200, 500 and 600 °C, respectively, *C* represents the calcination under air for 2 h at 400 °C. There were processes through the combination of LTR, HTR′, HTR and C. For example, HTR/C represents a reduction under hydrogen at 600 °C for 2 h and then a calcination under air at 400 °C for 2 h, HTR′/C/LTR represents a reduction at 500 °C, a calcination at 400 °C and finally a reduction at 200 °C. Moreover, WP represents the fresh Au-i/$K_2La_2Ti_3O_{10}$ without going through any pretreatment.

Table 1 lists the band gaps and the gold-crystal sizes of the fresh and each pretreated Au-i/$K_2La_2Ti_3O_{10}$. It can be found that all of the band gaps were close to that from $K_2La_2Ti_3O_{10}$, and were in the UV region. However, may be due to the influence from the plasma bands of gold in the visible region, these measured values slightly shifted toward the direction of visible light region. For the gold crystal sizes measured from XRD, all the pretreated samples possessed the sizes close to that (i.e., 50 nm) without any pretreatment. Nevertheless, it is noticed that the gold crystal sizes were larger than 50 nm, while the pretreatment at 600 °C reduction temperature (HTR) was carried out. On the other hand, the crystal sizes were less than 50 nm, while the other pretreatment processes (without HTR step) were carried out (either with calcination or lower temperature reduction). These results suggest that the pretreatment at the reduction temperature as high as 600 °C may enhance the aggregation of gold crystals on the surface of $K_2La_2Ti_3O_{10}$. However, the measured half maximum breadths of all Au-loaded samples were in a close range, some of the change of the Au crystal size shown in Table 1 were in the experimental error (i.e., ±3 nm) of this research. Moreover from XRD patterns, each pretreated sample possessed similar main phases and peak intensities as those of un-pretreated sample. This indicates that the pretreatment processes used in this research did not influence the crystallinity of $K_2La_2Ti_3O_{10}$ significantly.

Fig. 6 shows the UV–vis absorption bands from $K_2La_2Ti_3O_{10}$, the fresh Au-i/$K_2La_2Ti_3O_{10}$ (i.e., WP), and all the pretreated samples of Au-i/$K_2La_2Ti_3O_{10}$. It can be observed that for $K_2La_2Ti_3O_{10}$, there was no absorption band around 560 nm, which is corresponding to the plasma resonance on the surface of gold nano-particles. The absorption from gold on fresh Au-i/$K_2La_2Ti_3O_{10}$ (WP) was rather

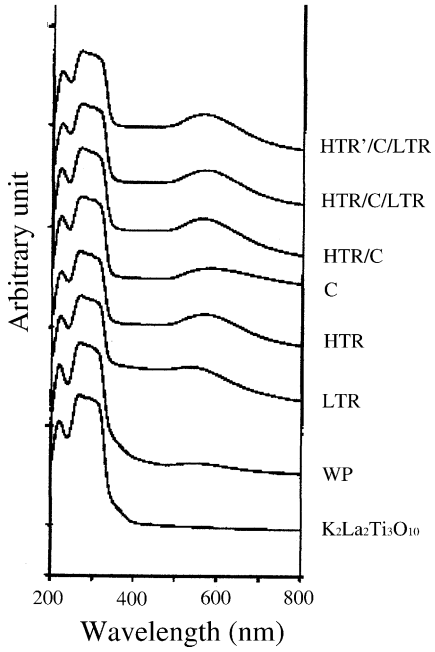

Fig. 6. UV–vis spectra of Au-i/$K_2La_2Ti_3O_{10}$ (1.1 wt.% Au) after different pretreatments. WP, without pretreatment; LTR, reduction under H_2 at 200 °C; HTR, reduction at 600 °C; HTR′, reduction at 500 °C and *C*, calcination under air at 400 °C.

weak. This indicates that most gold on WP sample was still in the form of ions, which can not provide plasma resonance. However, there were apparent absorptions from gold nano-particles on all the pretreated samples. Specially, strong absorptions from plasma resonance were observed for the samples reduced at high temperatures such as 500 or 600 °C.

The reaction activities for photo-catalytic water splitting on un-pretreated and all the pretreated Au-i/$K_2La_2Ti_3O_{10}$ under 300 nm UV light are listed in Table 1, while the initial rate for the production of hydrogen was calculated from the experimental data. It can be found that the un-pretreated sample (WP) possessed the lowest activity. This is due to the least gold metal and due to the largest amount of chloride poison on the surface of $K_2La_2Ti_3O_{10}$, suggested from the experimental results of UV-vis and TPR. A reduction of Au-i/$K_2La_2Ti_3O_{10}$ at 200 °C under hydrogen (LTR) can reduce most gold ions to nano gold metal; therefore, this can increase the reaction activity by three times. However, the samples through the only calcinations at 400 °C under air (*C*) or through the reduction at 600 °C under hydrogen (HTR or HTR/C) were slightly poorer than that under LTR. This may be due to the fact that the calcinations under air is not as effective as LTR for the reduction of gold ions, as shown in Fig. 6. For HTR, the reduction temperature was simply too high, the formation of larger gold particles caused the lower activity of this catalyst. Interestingly, HTR/C possessed the lowest activity among all the pretreated samples. The measured crystal size of gold on this sample was the smallest as shown in Table 1. The strong intensity of plasma resonance from this sample as shown in Fig. 6 indicates the complete

reduction of gold ions. Both should have been good for the reaction activity. Therefore, the low activity of the sample from HTR/C may suggest that the surface of nano-gold might contain oxygen or nitrogen after the reduction and air calcination, which increase the resistance for transferring the electron and hole generated in $K_2La_2Ti_3O_{10}$. On the other hand, when the sample (HTR/C) was treated under hydrogen at 200 °C again (HTR/C/LTR), although the removal of surface oxygen or nitrogen caused a slight increase of gold crystal size; however, the reaction activity was increased significantly.

It can be concluded that except the sample pretreated by HTR/C processes, in general, all the pretreated samples possessed an initial hydrogen production rate within a close range (more than 700 μmol/g/h). They all are significantly higher than the initial rate of 282 μmol/g/h from the (WP) sample without any pretreatment.

3.4. Comparison between Au-i/$K_2La_2Ti_3O_{10}$ and Ni/$K_2La_2Ti_3O_{10}$

It is well-known from Domen and coworkers [24,25] that $K_2La_2Ti_3O_{10}$ with 4.5 wt.%Ni (3 atom% Ni) and pretreated under reduction–oxidation processes possesses a high photo-catalytic activity under UV irradiation for water splitting. Therefore, nickel-loaded $K_2La_2Ti_3O_{10}$ was used as the bases for the comparison in this research. However, it is noticed that the light source for the photo-reaction system used by Domen et al. was different from ours. Mercury lamp with broad wavelength range (with UV and vis) was used in their studies, in contrast to narrow wavelength ranges (with only UV or only vis) used in ours. Therefore, the catalytic activities of nickel-loaded $K_2La_2Ti_3O_{10}$ were re-examined in our photo-reaction system, in order to have a fair comparison with those of $K_2La_2Ti_3O_{10}$ loaded with nano-gold.

$K_2La_2Ti_3O_{10}$ with 4.5 wt.%Ni (Ni/$K_2La_2Ti_3O_{10}$) and pretreated under reduction–oxidation processes was prepared in this research, according to the process presented by Domen and coworkers [24,25]. Au-i/$K_2La_2Ti_3O_{10}$ pretreated through the processes of HTR′/C/LTR was compared with this catalyst. Fig. 7 shows the reaction results, while irradiation under 300 and 420 nm light source were investigated, respectively. It can be observed that Ni/$K_2La_2Ti_3O_{10}$ catalyst was more active than Au-i/$K_2La_2Ti_3O_{10}$ under 300 nm UV irradiation. However, when the light source was changed to 420 nm (visible light), the hydrogen production rate from Au-i/$K_2La_2Ti_3O_{10}$ was more than that of Ni/$K_2La_2Ti_3O_{10}$. The reason for the better activity of Ni/$K_2La_2Ti_3O_{10}$ than that of Au-i/$K_2La_2Ti_3O_{10}$ under UV irradiation may be because the crystallinity of Ni/$K_2La_2Ti_3O_{10}$ was better than that of Au-i/$K_2La_2Ti_3O_{10}$ [34]. Due to the activities of both catalysts originated from the generation of electron and hole on $K_2La_2Ti_3O_{10}$, the slightly poorer crystallinity of Au-i/$K_2La_2Ti_3O_{10}$ would generate less electron and hole for the reaction. However, for the better reaction activity of Au-i/$K_2La_2Ti_3O_{10}$ than that

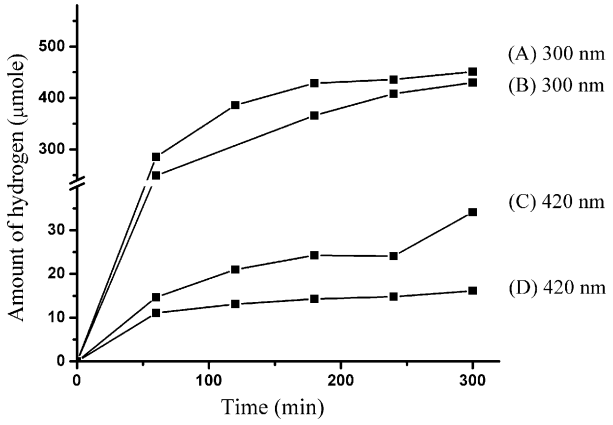

Fig. 7. Reaction time vs. hydrogen accumulated from photo-catalytic water splitting with 0.3 g each of (A) Ni/$K_2La_2Ti_3O_{10}$ (4.5 wt.% Ni) and (B) Au-i/$K_2La_2Ti_3O_{10}$ (1.1 wt.%Au) under 300 nm UV irradiation; (C) Au-i/$K_2La_2Ti_3O_{10}$(1.1 wt.% Au) and (D) Ni/$K_2La_2Ti_3O_{10}$(4.5 wt.% Ni) under 420 nm vis irradiation.

of Ni/$K_2La_2Ti_3O_{10}$ during the irradiation under visible light, the crystallinity of $K_2La_2Ti_3O_{10}$ should not be the main factor for the reaction. This is because the energy from the light source is much less than the band gap of $K_2La_2Ti_3O_{10}$. Therefore, it is proposed in this research that the plasma band generated on the surface of gold particles may be the main reason for the better reaction activity of Au-i/$K_2La_2Ti_3O_{10}$ under the irradiation of visible light. Although the light wavelength for the plasma resonance (around 520 nm) on gold is less than that of the light source (around 420 nm), it is believed that the anisotropic environment from the solid support caused a broad absorption from plasma resonance, which can overlap with the light source around 420 nm used in this research. This plasma resonance can polarize the electron distribution on nano-gold surface, which raise a probability for the electron transfer from gold to the conduction band of $K_2La_2Ti_3O_{10}$. Subsequently, this transferred electron and the hole generated on the metal surface cause the reduction and the oxidation of water splitting on the surface. On the other hand, there is only an absorption from d–d transition on nickel in the visible region, which is not sufficient for the transferring of electron from nickel to the surface of $K_2La_2Ti_3O_{10}$. Therefore, a higher reaction activity for water splitting occurred on Au-i/$K_2La_2Ti_3O_{10}$ than that on Ni/$K_2La_2Ti_3O_{10}$, under the irradiation of visible light.

4. Conclusions

It can be concluded from this research that nano-gold can enhance the reaction activity of $K_2La_2Ti_3O_{10}$ for the photo-catalytic water splitting. Au/$K_2La_2Ti_3O_{10}$ prepared through an incipient wetness impregnation process is better than that prepared through a deposition process, due to a better crystallinity of $K_2La_2Ti_3O_{10}$ was maintained. The pretreatment process for the reduction of gold ions to gold metal on

the surface is necessary for the enhancement of the reaction activity of $Au/K_2La_2Ti_3O_{10}$. Moreover, $Au/K_2La_2Ti_3O_{10}$ is less active for water splitting than $Ni/K_2La_2Ti_3O_{10}$ under UV irradiation; however, it is more active than $Ni/K_2La_2Ti_3O_{10}$ under vis irradiation.

Acknowledgement

We gratefully acknowledge the financial support from National Science Council in Taiwan.

References

[1] M. Haruta, T. Kobayashi, H. Sano, N. Yamada, Chem. Lett. (1987) 405.
[2] M. Haruta, N. Yamada, T. Kobayashi, S. Iijima, J. Catal. 115 (1989) 301.
[3] M. Haruta, S. Tsubota, T. Kobayashi, H. Kageyama, M.J. Genet, B. Delmon, J. Catal. 144 (1993) 175.
[4] J.-N. Lin, J.-H. Chen, C.-Y. Hsiao, Y.-M. Kang, B.-Z. Wan, Appl. Catal. B: Enviorn. 36 (2002) 19.
[5] J.-N. Lin, B.-Z. Wan, Appl. Catal. B: Enviorn. 41 (2003) 83.
[6] Y.-J. Chen, C.-T. Yeh, J. Catal. 200 (2001) 59.
[7] H.-S. Oh, J.H. Yang, C.K. Costello, Y.M. Wang, S.R. Bare, H.H. Kung, M.C. Kung, J. Catal. 210 (2002) 375.
[8] M. Haruta, M. Date, Appl. Catal. A: General 222 (2001) 427.
[9] G.C. Bond, D.T. Thompson, Catal. Rev. Sci. Eng. 41 (1999) 319.
[10] S. Link, Z.L. Wang, M.A. EI-Sayed, J. Phys. Chem. B 103 (1999) 3529.
[11] Y.-M. Kang, B.-Z. Wan, Catal. Today 35 (1997) 379.
[12] A. Fujishima, K. Honda, Nature 238 (1972) 37.
[13] K. Domen, A. Kudo, T. Onishi, J. Catal. 102 (1986) 92.
[14] K. Domen, A. Kudo, T. Onishi, N. Kosugi, H. Kuroda, J. Phys. Chem. 90 (1986) 292.
[15] A. Kudo, A. Tanaka, K. Domen, K. Maruya, K. Aika, T. Onishi, J. Catal. 111 (1988) 67.
[16] A. Kudo, K. Sayama, A. Tanaka, K. Asakura, K. Domen, K. Maruya, T. Onishi, J. Catal. 120 (1989) 337.
[17] K. Sayama, A. Tanaka, K. Domen, K. Maruya, T. Onishi, J. Phys. Chem. 95 (1991) 1345.
[18] K. Sayama, H. Arakawa, K. Domen, Catal. Today 28 (1996) 175.
[19] S. Ikeda, A. Tanaka, K. Shinohara, M. Hara, J.N. Kondo, K. Maruya, K. Domen, Microporous Mater. 9 (1997) 253.
[20] K. Sayama, K. Yase, H. Arakawa, K. Asakura, A. Tanaka, K. Domen, T. Onishi, J. Photochem. Photobiol. A: Chem. 114 (1998) 125.
[21] M. Kohno, S. Ogura, Y. Inoue, J. Mater. Chem. 6 (1996) 1921.
[22] M. Kohno, T. Kaneko, S. Ogura, K. Sato, Y. Inoue, J. Chem. Soc. Faraday Trans. 94 (1998) 89.
[23] S. Ogura, M. Kohno, K. Sato, Y. Inoue, Appl. Surf. Sci. 121 (1997) 521.
[24] T. Takata, K. Shinohara, M. Hara, J.N. Kondo, K. Domen, J. Photochem. Photobiol. A: Chem. 6 (1997) 45.
[25] S. Ikeda, M. Hara, J.N. Kondo, K. Domen, H. Takahashi, T. Okubo, M. Kakihana, Chem. Mater. 10 (1998) 72.
[26] K. Sayama, H. Arakawa, J. Photochem. Photobiol. A: Chem. 77 (1994) 243.
[27] K. Sayama, H. Arakawa, J. Photochem. Photobiol. A: Chem. 94 (1996) 67.
[28] A. Kudo, Catal. Surveys Asia 7 (2003) 31.
[29] T. Takata, A. Takata, M. Hara, J.N. Kondo, K. Domen, Catal. Today 44 (1998) 17.
[30] Handbook of Chemistry and Physics, 80th ed. CRC Press, 1999–2000, pp. 12–126.
[31] H.P. Klug, L.E. Alexander, X-ray Diffraction Procedures for Polycrystalline and Amorphous Materials, second ed, Wiley, New York, 1974.
[32] Y.-M. Kang, B.-Z. Wan, Appl. Catal. A: General 128 (1995) 53.
[33] S.D. Lin, M. Bollinger, M.A. Vannice, Catal. Lett. 17 (1993) 245.
[34] J.-S. Chen, Reduction of CO_2 in the Daily Life and Study of Layered Titanium Catalysts for Photo-Catalytic Water Decomposition. Master Thesis. National Taiwan University, 2000.